Phosphorylation of Forkhead Protein FoxO1 at S253 Regulates Glucose Homeostasis in Mice

Kebin Zhang,[1]* Xiaoqin Guo,[2]* Hui Yan,[1]* Yuxin Wu,[1,3] Quan Pan,[1] James Zheng Shen,[1] Xiaopeng Li,[1] Yunmei Chen,[1] Ling Li,[1] Yajuan Qi,[1] Zihui Xu,[1] Wei Xie,[2] Weiping Zhang,[1] David Threadgill,[1] Ling He,[4] Daniel Villarreal,[1] Yuxiang Sun,[1] Morris F. White,[5] Hongting Zheng,[2] and Shaodong Guo[1]

[1]Department of Nutrition and Food Science, College of Agriculture and Life Sciences, Texas A&M University, College Station, Texas 77843; [2]Xinqiao Hospital, Third Military Medical University, Chongqing 400037, China; [3]Queens University Belfast School of Biological Sciences, BT9 5AG Belfast, United Kingdom; [4]Division of Endocrinology, Department of Medicine, Johns Hopkins University, Baltimore, Maryland 04515; and [5]Division of Endocrinology, Children's Hospital Boston, Harvard Medical School, Boston, Massachusetts 02115

ORCiD numbers: 0000-0001-5126-731X (S. Guo).

The transcription factor forkhead box O1 (FoxO1) is a key mediator in the insulin signaling pathway and controls multiple physiological functions, including hepatic glucose production (HGP) and pancreatic β-cell function. We previously demonstrated that S256 in human FOXO1 (FOXO1-S256), equivalent to S253 in mouse FoxO1 (FoxO1-S253), is a key phosphorylation site mediating the effect of insulin as a target of protein kinase B on suppression of FOXO1 activity and expression of target genes responsible for gluconeogenesis. Here, we investigated the role of FoxO1-S253 phosphorylation in control of glucose homeostasis *in vivo* by generating global FoxO1-S253$^{A/A}$ knockin mice, in which FoxO1-S253 alleles were replaced with alanine (A substitution) blocking FoxO1-S253 phosphorylation. FoxO1-S253$^{A/A}$ mice displayed mild increases in feeding blood glucose and insulin levels but decreases in fasting blood glucose and glucagon concentrations, as well as a reduction in the ratio of pancreatic α-cells/β-cells per islet. FoxO1-S253$^{A/A}$ mice exhibited a slight increase in energy expenditure but barely altered food intake and glucose uptake among tissues. Further analyses revealed that FoxO1-S253$^{A/A}$ enhances FoxO1 nuclear localization and promotes the effect of glucagon on HGP. We conclude that dephosphorylation of S253 in FoxO1 may reflect a molecular basis of pancreatic plasticity during the development of insulin resistance. **(*Endocrinology* 160: 1333–1347, 2019)**

The forkhead protein forkhead box O1 (FoxO1) is an important transcription factor governing a variety of physiological function, including hepatic glucose production (HGP) and pancreatic β-cell function (1–3). Suppressed by insulin via activation of phosphatidylinositol 3-kinase (PI3K) and protein kinase B (Akt), FoxO1-stimulated HGP by gluconeogenesis is inhibited under feeding conditions, contributing to the maintenance of a steady level of blood glucose (4). Our previous studies demonstrated that the insulin receptor substrate 1 and 2 (Irs1 and Irs2) proteins are major mediators of insulin signaling cascades in activating endogenous PI3K

ISSN Online 1945-7170

Received 28 September 2018. Accepted 29 March 2019.
First Published Online 5 April 2019

*K.Z., X.G., and H.Y. contributed equally to this study.

Abbreviations: [^{14}C]2DG, 2-[^{14}C]deoxyglucose; A, alanine; A/+, heterozygous mice; A/A, homozygous mice; Akt, protein kinase B; BAC, bacterial artificial chromosome; EE, energy expenditure; EndoRa, endogenous glucose appearance; ES, embryonic stem; FBS, fetal bovine serum; FoxO1, forkhead box O1; G6pc, glucose-6-phosphatase; GIR, glucose infusion rate; GTT, gluocose tolerance test; HBSS, Hanks balanced salt solution; HGP, hepatic glucose production; HR, homologous recombination; IRS, insulin receptor substrate; KI, knockin; neo, neomycin; Pck, phosphenolpyruvate carboxykinase; PI3K, phosphatidylinositol 3-kinase; PTT, pyruvate tolerance test; RER, respiratory exchange ratio; Rg, glucose metabolic index; T2D, type 2 diabetes mellitus; VCO_2, rate of CO_2 output; VO_2, rate of O_2 consumption; WT, wild type; +/+, control or wild-type mice.

and Akt and subsequently suppressing FoxO1 in the liver in control of blood glucose homeostasis (5, 6). By contrast, upon loss of IRS1 and IRS2 genes, activation of PI3K and its downstream Akt were suppressed and subsequently failed to inhibit FoxO1-stimulated gluconeogenesis in the liver, promoting HGP, hyperinsulinemia, and diabetes mellitus (4–7). Thus, FoxO1 is required for the liver to develop hyperglycemic diabetes.

In hepatocytes, FoxO1 binds to the promoter region of glucose-6-phosphatase (G6pc) or phosphenolpyruvate carboxykinase (Pck)—two key metabolic enzymes—promoting the expression genes for gluconeogenesis and HGP (8). FoxO1 also binds to the insulin-responsive element on the promoter region of IRS2, increasing IRS2 gene transcription and insulin sensitivity (9). In the pancreas, early studies indicated that FoxO1 represses FoxA2-dependent Pdx1 transcription and β-cell apoptosis in IRS2-dependent manners (10). By contrast, it is recently shown that FoxO1 is involved in pancreatic β-cell differentiation and maintenance, whereas a loss of FoxO1 in pancreatic β-cell lineages can stimulate β-cell dedifferentiation into progenitor-like cells—even the α-cells—resulting in hyperglucagonemia (2).

FoxO1 is phosphorylated at S256 (human) by Akt, which primes phosphorylation of the other two sites at Thr24 and Ser319 (11, 12), enhances FoxO1 interaction with E3 ubiquitin ligase, and promotes FoxO1 nuclear export and/or degradation (13, 14), controlling expression of genes responsible for cellular growth, survival, and metabolism. Thus, FoxO1 is a key mediator of insulin and the Akt signaling pathway that controls multiple physiological functions (4). In addition to FoxO1-S256 phosphorylation by insulin and/or Akt, FoxO1 subcellular localization, transcriptional activity, and protein stability are modulated by multiple levels of post-translational modifications, including phosphorylation, ubiquitination, OGlcNacylation, and acetylation (1, 4). Given that FoxO1-S253 dephosphorylation, upon inactivation of Akt, is observed in tissues of diabetic animals, including the liver of db/db mice or mice lacking both IRS1 and IRS2 genes (6, 15), FoxO1 nuclear localization is a hallmark for the progression of type 2 diabetes mellitus (T2D), and dephosphorylation of FoxO1 at S253 (mice) is believed to be a potential indicator for FoxO1 activation that is associated with diabetes mellitus (4).

To explore further whether impairing FoxO1 phosphorylation at S253 itself is sufficient for the impairment of blood glucose homeostasis and insulin sensitivity *in vivo*, we generated FoxO1-S253$^{A/A}$ knockin (KI) mice, also referred to as A/A mice, in which the FoxO1 gene was expressed at its physiological level, and the endogenous FoxO1-S253 loci were replaced by alanine (A) to prevent FoxO1-S253 phosphorylation-mediated functionality. We analyzed the blood glucose and energy metabolism in the KI mice, and the role of FoxO1-S253 dephosphorylation in control of systemic glucose homeostasis was determined. In particular, we focus on liver and pancreas in this study to understand the regulation of FoxO1 by its S253 in control of energy metabolism at the bodily level.

Materials and Methods

Construction of FoxO1-S253$^{A/A}$ gene-targeting vector

To introduce a point mutation at S253 to alanine (S253A) in the endogenous FoxO1 genomic locus of mice, we first screened a PPCI-22 female 129S6/SvEvTac mouse bacterial artificial chromosome (BAC) library, provided by Roswell Park Cancer Institute (Buffalo, NY), with a FoxO1-specific probe. A BAC clone of a 200-kb DNA insert, containing FoxO1 genomic DNA, was obtained (Fig. 1A). A 4.2-kb fragment, spanning exon 2 of FoxO1, and a 3.2-kb fragment, spanning exon 3 of FoxO1, were amplified by PCR. The 4.2-kb fragment was amplified by PCR primer 1: 5′-ACCGCTCGAGGAAGCATCAGGAATGTGTCTGC-3′ with primer 2: 5′-AGGCGAGCTCGACCCTGTCTTTAATTACGTT-3′, and the 3.2-kb fragment was amplified by PCR primer 3: 5′-ACGGGGTACCTTATGTAACTCATCCCTACC-3′ with primer 4: 5′-TCGGGGTACCTATTTGCTAATTAACTTAGAC-3′. These two fragments were then cloned into upstream and downstream regions of the loxP-flanked neomycin (neo) cassette using *Xho*I and *Kpn*I linkers, respectively, in gene-targeting vector pPNT-2loxP (Fig. 1B) (5). Two-point mutations at S253 site were introduced by the change of two nucleotides from GT to AG with primer 5: 5′-CGGAGAAGAGCTGCAGCCATGGACAACAACAG-3′, which simultaneously created a *Pst*I site without changing any other amino acids. The *Pst*I site was used as a selection and genotyping marker for later gene-targeting vector validation, embryonic stem (ES) cell screening, and mouse offspring genotyping. The pPNT-FoxO1-S253A-targeting vector was successfully generated and validated by restriction endonuclease digestions with expected patterns.

Mouse ES cell transfection and Southern blotting

The linearized targeting vector pPNTFoxO1-S253A by *Not*I was used for ES cell transfection. To determine homologous recombination (HR), we picked 457 ES clones and examined them by the performance of Southern blot experiments. Different from many other negative clones (*e.g.*, clone 68), a positive clone 167 with both 5′ and 3′ HR near the neo cassette was identified using the ^{32}P-deoxy-CTP-labeled S5 probe and S3 probe, respectively (Fig. 1C and 1D). The S5 probe was amplified by PCR primer 6: 5′-CCTTCTCACAAGCACACTGGA-3′ with primer 7: 5′-GTGGGTGCTTTATGACAGAAG-3′, and the S3 probe was amplified by PCR primer 8: 5′-TCAGTAGAGTGTGCATTGTGC-3′ with primer 9: 5′-CTCACACACTGAGAACCATTG-3′, from the FoxO1 BAC clone. The neo cassette was removed by Cre

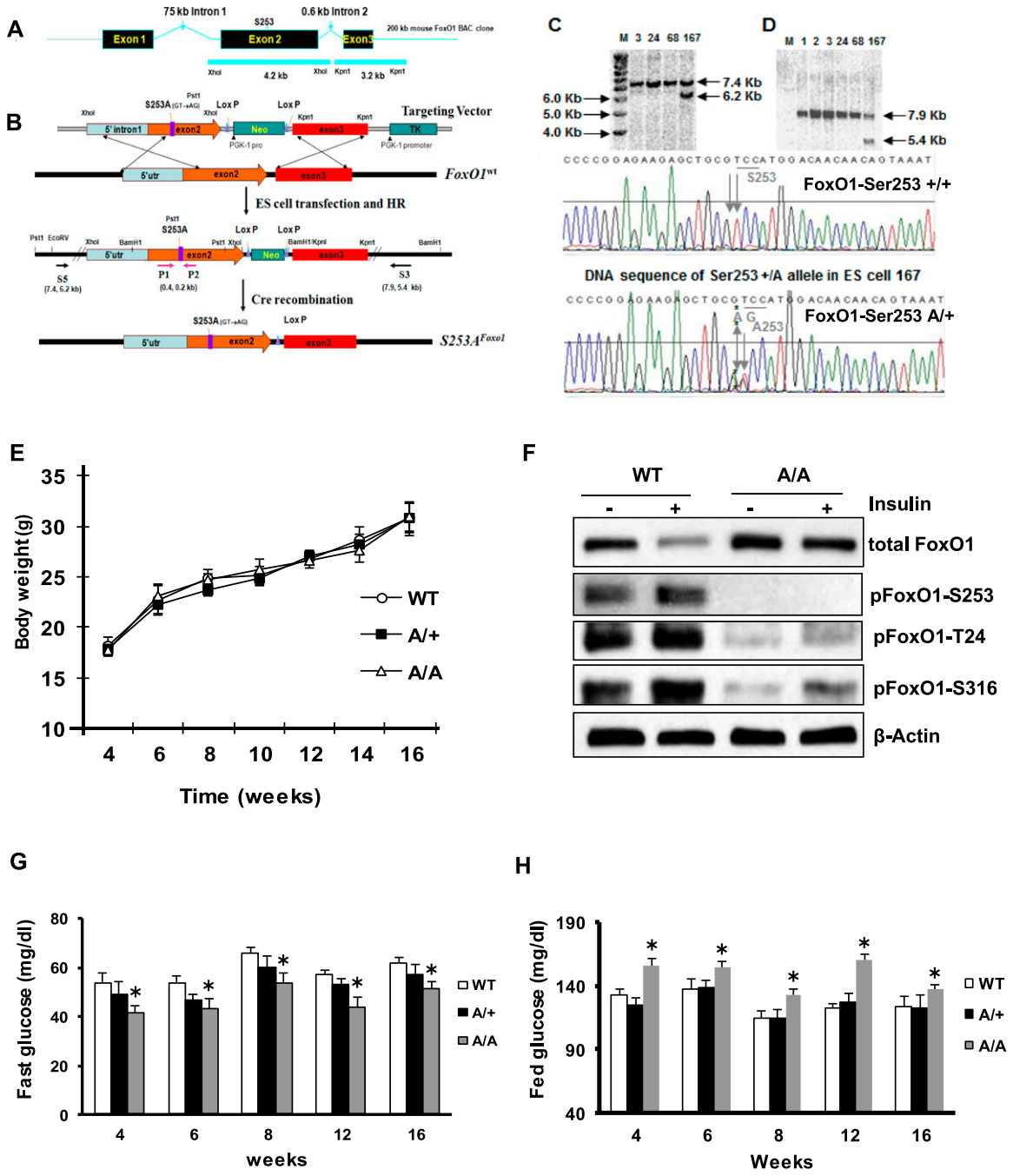

Figure 1. Generation of FoxO1-S253$^{A/A}$ mice and postprandial hyperglycemia. (A) The genomic locus of FoxO1 in mouse genome. (B) Gene-targeting strategy for generation of FoxO1-S253A mutation via embryonic stem (ES) cell and homologous recombination (HR). (C and D) Southern blot was performed for screening the 5′- and 3′-end HR in FoxO1 genomic loci. DNA sequencing of endogenous FoxO1 loci of negative and positive ES cells. (E) Body weight curve of mice of control wild-type (WT), heterozygous (A/+), and homozygous (A/A) mice at the ages of 4 to 16 weeks. (F) Effect of insulin on FoxO1 protein and phosphorylation (p) in hepatocytes. Primary hepatocytes were isolated from the control and A/A mice and treated with 100 nM insulin for 30 minutes, and 100 μg protein of cell lysates was subjected to Western blot against the antibody of FoxO1, T24, S316, and β-actin. (G and H) Blood glucose levels were measured in WT, A/+, and A/A mice at the ages 4 to 16 weeks during (G) 16 hours fasting and (H) random-fed conditions. *$P < 0.05$ vs WT and A/+ mice, n = 10 mice per group. M, Marker; Neo, neomycin; PGK-1, phosphoglycerate kinase 1; TK, thymidine kinase; utr, untranslated region.

expression (Fig. 1B). The FoxO1-S253$^{A/+}$ heterozygous allele in the DNA of the 167 ES clone was further confirmed by verification of a 600-bp fragment that was amplified by PCR primer 10: 5′-AGTGCTGCACTTCTAACATAC-3′ with primer 11: 5′-GAGAGAAGGTTGAGATTATCC-3′. The *Pst*I digestion of the 600-bp fragment produced a 400- and a 200-bp fragment from the S253A allele. With the use of primer 10 as a DNA sequencing primer, we further confirmed that the 600-bp fragment from the positive 167 ES cell clone contained both wild-type (WT) S253 allele (GT) and S253A allele (AG), whereas the 600-bp fragment from the negative 68 ES clone only contained two WT S253 alleles (GT).

Generation of FoxO1-S253$^{A/A}$ mutant mice and genotyping

The positive 167 ES clone was used for pronuclear injection in a fertilized mouse egg that was then transferred into two foster female mice. Two chimeric mice were generated, and the backcrossing of the chimeric mice to C57/BL6 mice generated 10 F1 offspring pups. The genotyping of the F1 offspring confirmed the germline transmission of the FoxO1-S253A allele. The mating of the male with the female heterozygous FoxO1-S253$^{A/+}$ allele (A/+ mice) generated the F2 offspring mice homozygous FoxO1-S253$^{A/A}$ allele (A/A mice) and WT FoxO1-S253$^{+/+}$ control mice (+/+ mice). All mice were with C57/BL6 and 129 Sv mixed background maintained on regular chow (Prolab Isopro 5P76). Male mice, ~8 to 12 weeks old, were analyzed if not specified in the legend. All animal protocols were approved by the Texas A&M University Institutional Animal Care and Use Committee.

Chemicals and antibodies

Insulin and glucagon were purchased from Sigma. Antibodies against FoxO1 [catalog no. 2880; Cell Signaling Technology (16), Danvers, MA], phosphorylated FoxO1-Thr24 [catalog no. 2599; Cell Signaling Technology (17)], phosphorylated FoxO1-S253 [catalog no. 9461; Cell Signaling Technology (18)], phosphorylated FoxO1-Ser316 [catalog no. 2486; Cell Signaling Technology (19)], glyceraldehyde 3-phosphate dehydrogenase [catalog no. 2118; Cell Signaling Technology (20)], β-actin [catalog no. 4970; Cell Signaling Technology (21)], and histone H1 antibody [catalog no. sc-8030; Santa Cruz Biotechnology (22), Dallas, TX] were used for Western blot.

Blood chemistry and metabolic analysis

Serum samples were analyzed for insulin and glucagon (Crystal Chem, Elk Grove Village, IL) and albumin (BioAssay Systems, Hayward, CA), using commercial protocols and reagents. Blood glucose levels were measured using a glucometer (Bayer, Leverkusen, Germany). For the glucose tolerance test (GTT), mice were unfed overnight and IP injected with 2 g D-glucose/kg body weight. For the pyruvate tolerance test (PTT), the unfed mice were injected IP with 2 g pyruvate/kg body weight. *In vivo* insulin stimulation was carried out in mice that were unfed and deeply anesthetized. Serum insulin and glucagon were measured with commercial kits (Crystal Chem). Hepatic glycogen concentration was analyzed, as previously described (5, 8). For glucagon tolerance tests, the 18-hour unfed mice were IP injected with glucagon, with a dose of 16 μg/kg body weight, and blood glucose was measured with a glucometer (Elite XL; Bayer, Whippany, NJ). The dose of glucagon was used, as recently described (23).

Hyperinsulinemic-euglycemic clamp of mice

Catheters were implanted in a carotid artery and a jugular vein of mice for sampling and IV infusions, 5 days before hyperinsulinemic-euglycemic clamp, when mice were at conscious states, as previously described (5, 24). Blood glucose was clamped at 150 mg/dL using a variable glucose infusion rate (GIR). Mice received washed erythrocytes from donors to prevent the loss in hematocrit that would otherwise occur. At 120 minutes, the clamp was sustained, and a 1-mCi bolus of 2-[^{14}C]deoxyglucose ([^{14}C]2DG) was administered. Blood was taken at 122 to 155 minutes for [^{14}C]2DG determination. Mice were anesthetized after the last sample, and tissues were excised. Plasma and tissue radioactivity of [3-^{3}H]glucose, [^{14}C]2DG, and [^{14}C]2DG-6-phosphate were determined, as previously described (24). Glucose appearance, endogenous glucose appearance (EndoRa), and glucose disappearance rates were determined using nonsteady-state equations (24). The glucose metabolic index (Rg) was calculated as described (24).

Indirect calorimetry measurements

Mice (12 weeks old) were acclimated in metabolic cages (TSE Phenomaster, Chesterfield, MO) for 2 days of adaptation. After 2 days of housing, mice were recorded for 3 minutes every hour for 2 consecutive days with the following measurements: gas exchange [rate of O_2 consumption (VO_2) and rate of CO_2 output (VCO_2)], food intake, and physical activities. Energy expenditure (EE) was calculated according to the manufacturer's manual. Values were normalized by body weight to the power of 0.75. The respiratory exchange ratio (RER) was estimated by calculation of the ratio of VCO_2/VO_2 (25).

Pancreas immunohistochemistry, morphometric, and chemical analyses

Pancreases from WT and A/A mice were fixed in 10% formalin overnight and then processed for paraffin embedding. Tissues from five mice of each genotype were sectioned to a thickness of 5 μm used for morphometric and immunohistochemical analysis. For morphometric analysis, at least three pancreatic sections from three to five mice of each genotypes were staining with hematoxylin and eosin and scanned on the Aperio ScanScope (Leica, Wetzlar, Germany). Islet cross-sectional area and total pancreatic area were measured using ImageJ software (National Institutes of Health, Bethesda, MD) and calculated as the ratio of islet/total pancreas. Quantification of the number of pancreatic α- and β-cells was calculated using coimmunofluorescence staining with an antibody of insulin or glucagon from a nonoverlapping field on a Leica confocal microscope. The total numbers of glucagon- or insulin-positive cells were counted from pancreatic sections immunostained for glucagon and insulin, respectively.

Total insulin and glucagon in the pancreas were extracted from the whole pancreas by acid-ethanol extraction, according to the Animal Models of Diabetic Complications Consortium protocol (https://www.diacomp.org/shared/document.aspx?id=73&docType=Protocol). Pancreatic insulin and glucagon levels were determined by the Bio-Plex mouse diabetes immunoassay (Bio-Rad Laboratories Inc., Hercules, CA), as described (26).

Pancreatic islet isolation, islet insulin, and glucagon content and glucose-stimulated insulin secretion

Islets were collected using the collagenase method and cultured overnight in low-glucose RPMI-1640 medium using our previous protocols (27). In brief, 3 mL of 1 mg/mL collagenase P, dissolved in ice-cold Hanks balanced salt solution (HBSS), was injected via the pancreatic duct, and the common bile duct near the liver was clamped. Once inflated, the pancreas was excised and placed in a 50-mL tube with 3 mL collagenase P solution. Tubes containing digest were placed in a 37°C water bath at 100 to 120 shaking/min for 10 to 12 minutes.

Subsequently, 10% fetal bovine serum (FBS) solution was added to digest tubes to stop collagenase P activity. The islets were then centrifuged using a Ficoll gradient Histopaque-1077 (Sigma-Aldrich, Kawasaki, Japan), per the manufacturer's instruction. Islets were then collected from the gradient, washed with HBSS, and handpicked using a 200-μL pipette under a dissection microscope. The hand-picked islets were then suspended in RPMI-1640 medium and incubated overnight in RPMI-1640 medium containing 10% FBS, 100 U/mL penicillin, 100 μg/mL streptomycin, 10 mM Hepes, 2 mM L-glutamine, 1 mM sodium-pyruvate, 0.05 mM 2-mercaptoethanol, and 5.5 mM glucose. The next day, each islet was transferred to a 12-well plate (~10 islets per well) and cultured with 1 mL of the HBSS medium, pH 7.2, consisting of 114 mM NaCl, 4.7 mM KCl, 1.2 mM KH_2PO_4, 1.16 mM $MgSO_4$, 20 mM HEPES, 2.5 mM $CaCl_2$, 25.5 mM $NaHCO_3$, 0.2% BSA, and 3.3 mM glucose for 2 hours. Following the 3.3-mM glucose incubation, islets then were incubated in either 3.3 mM or 22.2 mM glucose for another 2 hours. The 10- or 50-μL of the HBSS buffer was collected for insulin and glucagon measurement, respectively, using a mouse insulin or glucagon ELISA kit (Mercodia, Uppsala, Sweden).The islets were collected for insulin and glucagon measurement using Bio-Plex mouse diabetes immunoassay (Bio-Rad Laboratories Inc.), as described (26), and normalized to the islet protein content.

Real-time quantitative PCR analysis

RNA was extracted with TRIzol reagent (Invitrogen, Carlsbad, CA) (28). RNA (1 μg) was used as a template for cDNA synthesis, using the SuperScript first-strand synthesis system (Bio-Rad Laboratories Inc.). The quantity of cDNA for each transcript was measured using real-time PCR with SYBR Green Supermix (Bio-Rad Laboratories Inc.). Relative quantitative analysis was performed by calculation of the ratio of the mRNA amount for the gene of interest over the amount of internal control cyclophilin with duplicate samples. The PCR primers were described previously (8).

Primary hepatocyte isolation and culture and hepatic glucose production assay

Primary hepatocytes were isolated from mice and cultured in DMEM medium, as described previously (8). For HGP assay, freshly isolated hepatocytes were cultured in DMEM with 2% FBS. After 3 hours of attachment, cells were cultured in HGP buffer (120 mM NaCl, 5.0 mM KCl, 2.0 mM $CaCl_2$, 25 mM $NaHCO_3$, 2.5 mM KH_2PO_4, 2.5 mM $MgSO_4$, 10 mM HEPES, 0.5% BSA, 10 mM sodium DL-lactate, and 5 mM pyruvate, pH 7.4) and treated with chemicals. Culture medium was collected to determine the glucose concentration, using the Amplex Red glucose assay kit (Invitrogen). For glycogenolysis assays, the sodium DL-lactate and pyruvate were removed from the HGP buffer, and then medium glucose contents were determined; gluconeogenesis involves subtraction of medium glucose of HGP by glycogenolysis.

Western blot and immunoprecipitation

Tissue or cellular protein lysates were prepared, resolved by SDS-PAGE, and transferred to nitrocellulose membrane for immunoblotting analysis using specific antibodies. Signal intensity was measured and analyzed by National Institutes of Health ImageJ software, as previously described (8, 28).

Statistical analysis

All results are presented as means ± SEM, determined by two-tailed Student *t* tests or one-way ANOVA. Paired comparisons of the means were made, and $P < 0.05$ was defined as statistical significance. The Bonferroni method was used to adjust the observed significance levels for testing of multiple contrasts (5, 8).

Results

Generation of FoxO1-S253$^{A/A}$ mutant mice

We generated mice with an alanine point mutation at S253 (S253A; or A allele) in FoxO1 genetic loci (Fig. 1A–1D). We bred the male and female A/+ mice to generate WT (or +/+), heterozygous (A/+), and homozygous (A/A) mice for the FoxO1-S253 allele, achieving a Mendelian ratio of 1:2:1, respectively. All of the mice appeared healthy, ruling out the possibility that homozygous FoxO1-S253$^{A/A}$ alleles are embryonic lethal. Initial analysis indicated that body weight of the A/+ and A/A mice was not significantly changed by the age of 16 weeks (Fig. 1E). The serum albumin levels were measured, and there were no significant differences between WT and A/A mice (3.4 ± 0.21 g/dL WT vs 3.5 ± 0.26 g/dL A/A) in the feeding state nor between the groups in the fasting state, indicating that the FoxO1-S253A mutation did not cause liver damage.

FoxO1-S253$^{A/A}$ mutation enhances FoxO1 stability *in vivo*

We next examined the levels of total FoxO1 protein in the primary hepatocytes of the mice. Insulin stimulated phosphorylation of FoxO1 at T24, S253, and S316 and reduced total FoxO1 protein level by 60% in WT hepatocytes, analyzed by immunoblotting. However, insulin failed to induce FoxO1 degradation in S253$^{A/A}$ primary hepatocytes, and the basal level of total FoxO1 increased in the mutant cells (Fig. 1F). As expected, the FoxO1-S253 phosphorylation by insulin stimulation was diminished in A/A hepatocytes, and the other two sites of phosphorylation at T24 and S316 were also largely impaired (Fig. 1F). Together, these data confirmed that S253 is a key site in control of FoxO1 stability and phosphorylation at the other two sites *in vivo*.

Glucose homeostasis of FoxO1-S253$^{A/A}$ mice

To evaluate *in vivo* function of FoxO1-S253 in glucose homeostasis, we measured blood glucose concentrations of WT, A/+, and A/A mice at overnight fasting or random-fed states. Blood glucose, under fasting conditions in the A/A mice, was significantly decreased by 16% to 25% compared with that of control mice (Fig. 1G). However, blood glucose under feeding conditions showed a 15% to 30% increase in the A/A mice

compared with that of the control mice at the age of 4 to 16 weeks ($P < 0.05$; Fig. 1H). There was no significant difference between +/+ and A/+ mice (Fig. 1G and 1H).

Insulin sensitivity of FoxO1-S253$^{A/A}$ mice

We next examined the insulin sensitivity of control and A/A mice by the performance of hyperinsulinemic-euglycemic clamp analysis and the GTT. Upon peripheral insulin infusion (2.5 mU · kg^{-1} · min^{-1}), the circulating glucose concentrations were maintained at 150 mg/dL in both control WT and A/A mice. The GIR in KI mice had no significant differences (Fig. 2A). Basal EndoRa for HGP in KI mice displayed a lower level without significance compared with WT mice under the hyperinsulinemic condition (Fig. 2B). The Rg for glucose uptake in soleus muscle and hearts was in trend to decrease but insignificantly and unchanged in the gastrocnemius and vastus lateralis muscle and white adipose tissue (Fig. 2C and 2D), suggesting that A/A barely affected glucose uptake in muscle and white adipose tissues.

We next performed the GTT; KI mice did not display glucose intolerance upon glucose injection (Fig. 2E). However, KI mice were hyperinsulinemic in that serum insulin levels increased significantly in A/+ by twofold and A/A mice by threefold (WT: 0.4 ± 0.07 ng/mL, A/+: 0.78 ± 0.03 ng/mL vs A/A: 1.2 ± 0.08 ng/mL) in the fasting state (Fig. 2G). A similar effect was also observed in the feeding condition (WT: 0.8 ± 0.02 ng/mL, A/+: 1.1 ± 0.03 ng/mL vs A/A: 1.6 ± 0.02 ng/mL; Fig. 2F). KI mice also showed high insulin release upon the GTT (Fig. 2G). These indicated that the insulin sensitivity was actually reduced in KI mice.

We next performed the PTT, and both A/+ and A/A mice exhibited pyruvate intolerance (Fig. 2H). We next measured serum glucagon levels in these mice. Compared with WT mice, glucagon concentrations decreased in A/A mice by 50% during the fasting state (WT: 118 ± 10 pmol/mL vs A/A: 60 ± 5 pmol/mL, $P < 0.05$), as well as in the feeding condition (WT: 50 ± 4.3 pg/mL vs A/A: 32 ± 3.1 pg/mL; Fig. 2I). Additionally, KI mice exhibited increases by nearly 1.5-fold in expressions of *Pck1* or *G6pc* in the liver when mice were at either feeding or fasting state (Fig. 2J). These data indicate that A/+ and A/A mutations affect gluconeogenesis, blood insulin, and glucagon levels.

VO_2 and EE in FoxO1-S253$^{A/A}$ mice

We also measured food intake, physical activity, and EE by the analysis of VO_2 and VCO_2 in mice in the metabolic cages. WT and A/A mice exhibited no difference in food intake (Fig. 3A), but physical activity was significantly reduced in A/A mutant mice in the dark phase (Fig. 3B). Meanwhile, VO_2 and EE were higher in A/A mice, in particular, during the dark phase (Fig. 3C and 3D). The RER—the ratio between the amount of VCO_2 and VO_2 —had no significant changes between A/A and control mice (Fig. 3E). The results indicate that A/A mutant mice have higher metabolic rates, even though the physical activities were reduced.

Islet morphology of FoxO1-S253$^{A/A}$ mice

The serum insulin level increases, whereas the glucagon level reduces in A/A mice, and thus, we suspect that these changes in pancreatic hormones may reflect a remodeling of β-cells and α-cells in the pancreas. To examine this possibility, pancreases were isolated from WT and A/A mice. We measured pancreatic hormone contents and performed immunohistochemical and morphometric analysis. A/A mice exhibited a 41% higher pancreas weight than WT mice (Fig. 4A). Insulin contents were increased by 50% in the pancreas and by 52% in the islets of A/A mice, whereas glucagon contents were decreased by 38% in the pancreas and by 40% in the islets of A/A mice compared with that of WT mice ($P < 0.05$; Fig. 4B–4E). We further investigated the insulin or glucagon releases in the islets isolated from these mice. KI mice showed increased insulin secretion and decreased glucagon secretion (Fig. 4F and 4G). Immunostaining of the pancreas by glucagon and insulin revealed a 36.8% reduction of glucagon-positive α-cells in islets from A/A mice, but insulin-positive β-cells were unchanged in both genotypes (Fig. 4H–4J). We also found that WT islets had 2.30% ± 0.29% insulin and glucagon double-positive cells, whereas A/A islets exhibited 4.40% ± 0.06% double-positive cells in the pancreas ($P < 0.01$, n = 3 mice per group). The ratio of α-cells to β-cells in each islet was reduced by 27.7% in A/A mice compared with WT ($P < 0.05$; Fig. 4K). Based on quantification of the islet area on hematoxylin and eosin staining, the percentage of the islet area relative to total pancreas area was reduced by 41.9% in A/A mice (Fig. 4L and 4M). With the consideration of the 41.4% increase in pancreatic weight (Fig. 4A), the total islet mass did not change in A/A mice compared with WT mice. We further measured gene expression for markers, which are responsible for different stages of pancreatic differentiation (3). The pancreas of A/A mice exhibited a significant increase in the expression of the progenitor cell markers, including Sox9, Sox17, and Hnf1b, and marked decreases in expression of acinar cell markers, such as Amy2a, Cela1, and Ptf1a, suggesting that the A mutation of Foxo1-S253 might increase progenitor cell and reduce acinar cell differentiation in the pancreas (Fig. 4N). For β-cell markers, A/A significantly increased Neurod1 and

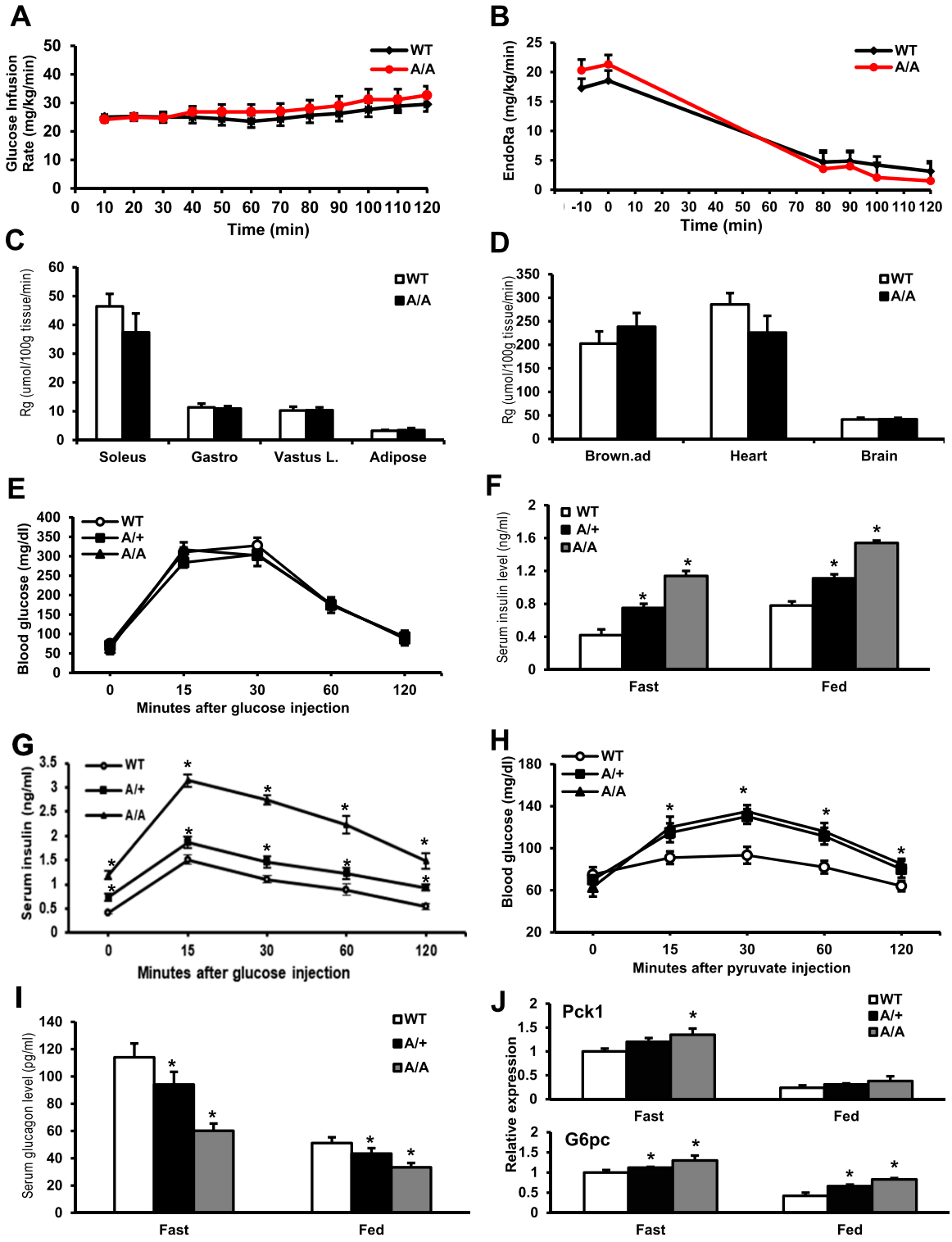

Figure 2. FoxO1-S253$^{A/A}$ mice exhibit impaired insulin and glucagon secretion and glucose homeostasis. (A) GIR of control and A/A mice at the ages of 16 weeks in hyperinsulinemic-euglycemic clamp assays; n = 8 mice per group. (B) HGP of mice during the clamp assay. (C and D) Glucose uptake in a variety of tissues of mice during the clamp assay. $P < 0.05$, n = 8 mice per group. (E) GTTs were performed in 10-week mice (n = 6) under a 16-hour fasting condition. Blood glucose was plotted against the time after the IP 2-g D-glucose/kg body weight glucose injection. (F) Serum insulin concentration was measured in mice during 16-hour fasting and random-fed states. *$P < 0.05$ vs WT mice, n = 10 mice per group. (G) Serum insulin concentration was measured in mice during the GTT from (E). *$P < 0.05$ vs WT mice, n = 10 mice per group. (H) PTTs were conducted in unfed mice after 16 hours overnight. Blood glucose levels (means ± SEM, n = 6 mice per group) were determined at the indicated time points after an IP injection of 2 g pyruvate/kg body weight. *$P < 0.05$ vs WT. (I) Serum glucagon concentration was measured in mice during the 16-hour fasting and random-fed states. *$P < 0.05$ vs WT mice, n = 10 mice per group. (J) Expression of Pck1 and G6pc in the liver of WT, A/+, and A/A under a 16-hour fasting or random-fed condition. *$P < 0.05$ vs WT, n = 6. Brown.ad, brown adipose; Gastro, *gastrocnemius*; Vastus L., *vastus lateralis*.

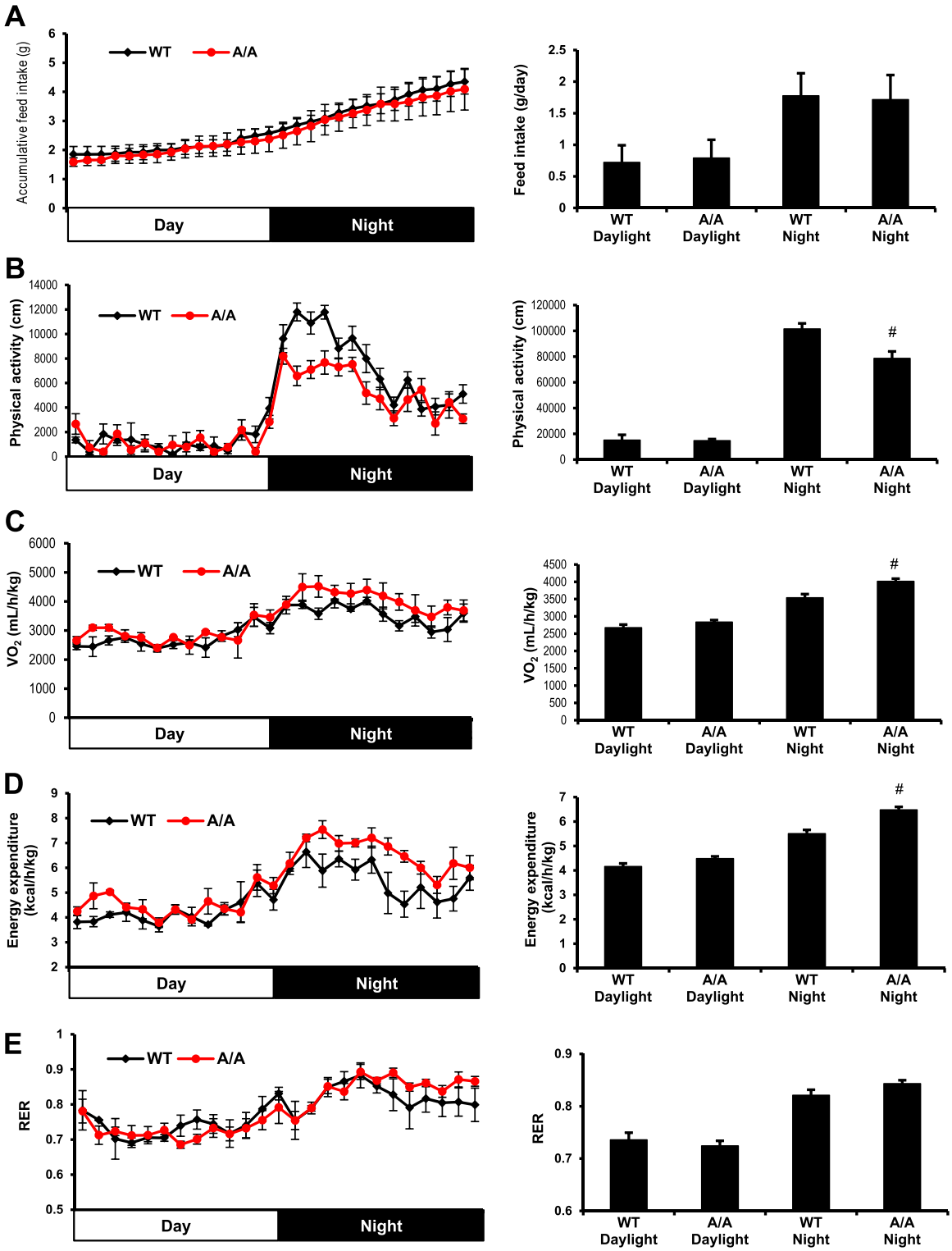

Figure 3. EE increases in FoxO1-S253$^{A/A}$ mice. The mice at the age of 16 weeks old were placed in metabolic cages for the measurement of food intake, physical activity, and VO_2, and EE. (A) Food intake, (B) physical activity, (C) VO_2, (D) EE, and (E) RER were calculated. $^{\#}P < 0.05$ vs WT, n = 8 mice per group.

MafA expression in the whole pancreas (Fig. 4N) and significantly increased expression of insulin, Neurod1, and Pdx1 in the islets of the pancreas (Fig. 4O). For α-cell markers, A/A significantly decreased expression of Arx, Loxl4, Hmgb3, and Fev mRNA expression in the whole pancreas (Fig. 4N) and significantly decreased expression of glucagon and Fev expression in islets (Fig. 4O). Although the mRNA of acinar cell and progenitor cell markers, such Amy2a, Cela1, Sox17, and Hnf1b, was also detected in isolated islets, the expression level of

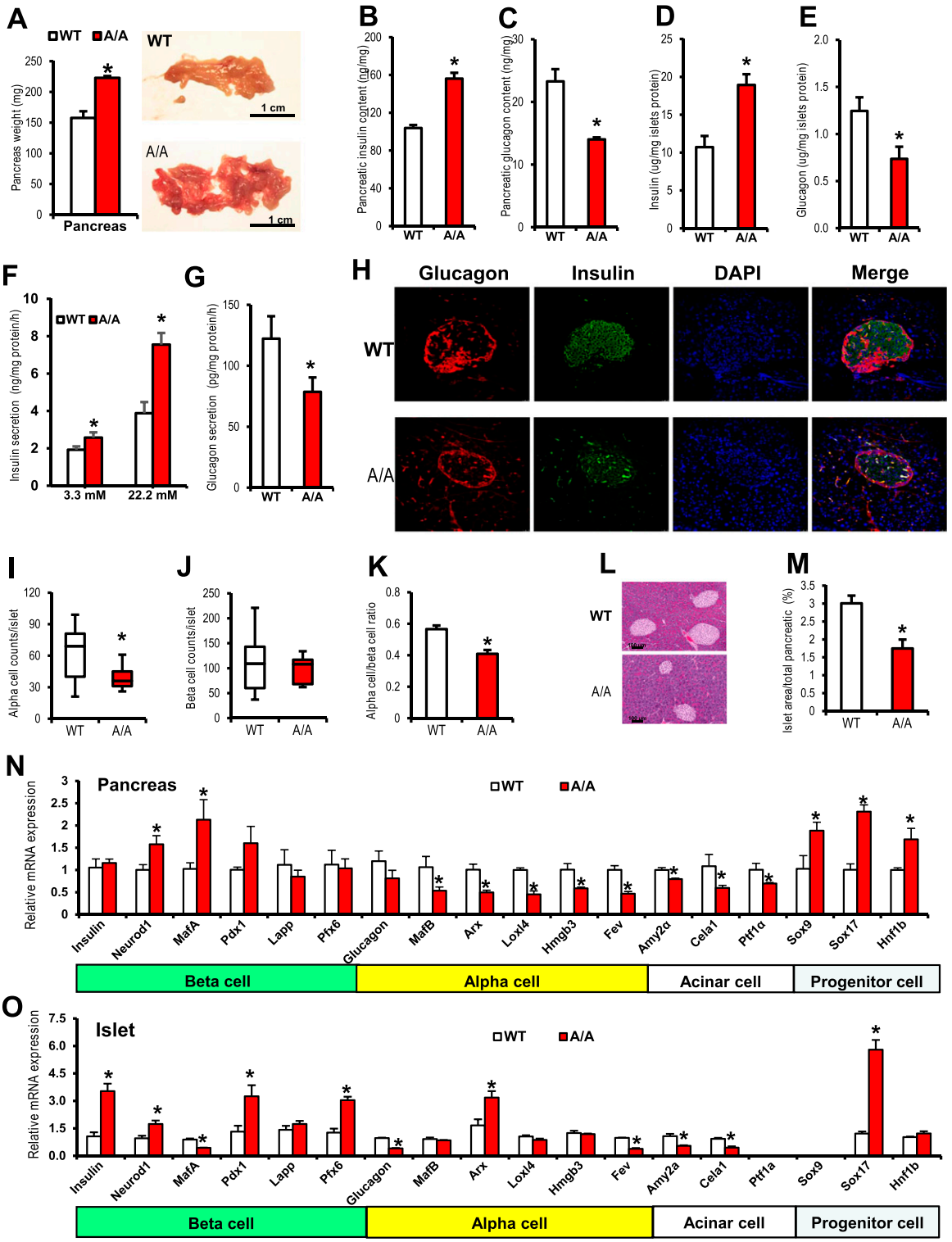

Figure 4. FoxO1-S253$^{A/A}$ mice exhibit impaired α-cells, insulin, and glucagon synthesis in the pancreas. (A) Representative pancreas of control (WT) and A/A mice at the age of 12 weeks at random-fed states. *$P < 0.05$ vs WT, n = 6. (B and C) Insulin and glucagon concentration was measured in the pancreas of control and A/A mice at the age of 12 weeks at random-fed states. *$P < 0.05$ vs WT, n = 3. (D and E) Insulin and glucagon concentration was measured in the islets of control and A/A mice and normalized by islet protein. *$P < 0.05$ vs WT, n = 3. (F) Insulin secretion from the islets isolated from control and A/A mice. *$P < 0.05$ vs WT, n = 3. (G) Glucagon secretion from the islets isolated from control and A/A mice under 3.3 mM glucose condition. *$P < 0.05$ vs WT, n = 3. (H) Immunostaining of pancreas from 16-week-old random-fed mice by glucagon and insulin. Representative images are shown. *$P < 0.05$ vs WT, n = 6 mice per group. (I–K) The number of (I) α-cells and (J) β-cells was counted from at least three mice per group, and the (K) ratio of α-cell/β-cell number in each islet was counted and calculated. *$P <$ 0.05 vs WT, n = 3 mice per group. (L) The representative images of the pancreas and islets of WT and A/A mice. (M) The area of islets in total pancreas was calculated in WT and A/A mice. *$P < 0.05$ vs WT, n = 4. (N and O) The expression of marker genes responsible for the pancreatic β-cell, α-cell, acinar cell, and progenitor cell in (N) total pancreas or (O) islets isolated from WT and A/A mice. *$P < 0.05$ vs WT, n = 3. DAPI, 4′,6-diamidino-2-phenylindole.

these genes in the islet was 10^3 times less than those in the whole pancreas (data not shown). Collectively, these data suggest that the A/A pancreas has a reduced α-cell number, which may result from reduced progenitor cell differentiation.

Taken together, these data suggest that the A/A pancreas may inhibit progenitor cell differentiation into endocrine cells and increase the pancreatic mass. Moreover, it probably impairs differentiation of α-cells and leads to decreased glucagon levels in both serum and pancreas.

Glycogen metabolism in FoxO1-S253$^{A/A}$ mice

We next measured liver glycogen contents, as both insulin and glucagon control glycogen levels contribute to blood glucose homeostasis in the fasting and feeding state. Consistent with increased blood insulin and decreased glucagon levels, the glycogen concentrations in the liver of unfed A/A mice were 81.5% higher than that of unfed WT mice, whereas there were no significant changes in the liver of fed WT and A/A mice (Fig. 5A). These data suggested that glycogenolysis in the liver of unfed A/A mice was inhibited, probably by the elevation of insulin level, whereas such an effect was diminished in the feeding state.

HGP of FoxO1-S253$^{A/A}$ in response to glucagon

We further examined whether FoxO1-S253A impairs glucagon-stimulated glucose production in mice. During the feeding state, glucagon enhanced blood glucose by 25% in WT mice and 35% in A/A mice (Fig. 5B). The glucagon tolerance test indicated that A/A mice displayed higher blood glucose concentrations when glucagon was injected after 15 minutes, an effect sustained up to 60 minutes (Fig. 5C). We further examined whether the effect of A/A on HGP is mediated by gluconeogenesis or glycogenolysis in cells. The primary hepatocytes were isolated from WT and A/A mice, and HGP was analyzed *in vitro* by the measurement of glucose release in the cultured medium by hepatocytes. In the basal condition, A/A hepatocytes exhibited a 50% higher HGP and 47% higher gluconeogenesis compared with WT cells (Fig. 5D and 5E). Upon glucagon stimulation, A/A hepatocytes also had a 47% higher HGP and 51% higher gluconeogenesis compared with WT cells (Fig. 5D and 5E). The fold change of gluconeogenesis by glucagon in WT cells (1.4-fold induction) was not statistically different from that in A/A cells (1.5-fold; Fig. 5E). These data indicated that the S253A mutation induced the basal level of HGP, and gluconeogenesis and glucagon-stimulated gluconeogenesis were not impaired. The higher response of A/A mice to the exogenous glucagon stimulation in blood glucose may result from a higher concentration of hepatic glycogen and associated glycogenolysis in A/A mice.

Glycogenolysis increased in both WT and A/A hepatocytes in response to glucagon stimulation, similar to the basal level of A/A cells (Fig. 5E). In agreement with the HGP assay, gene-expression analyses indicated that glucagon-induced G6pc gene expression significantly increased by nearly twofold in A/A cells, similar to the twofold increase in control hepatocytes in response to glucagon stimulation (Fig. 5F).

FoxO1-S253$^{A/A}$ increases glucagon-stimulated FoxO1 nuclear translocation

Finally, we determined whether glucagon affects FoxO1 nuclear translocation and examined the effect of A/A in the primary hepatocytes. Glucagon induced FoxO1 nuclear translocation by 1.4-fold in WT hepatocytes. However, FoxO1 nuclear translocation markedly increased by 2.2-fold in A/A hepatocytes vs WT cells. In response to glucagon stimulation, nuclear FoxO1 increased by 25% in A/A hepatocytes compared with the nontreatment of A/A cells ($P < 0.05$; Fig. 5G).

Discussion

In this study, we generated a FoxO1-S253$^{A/A}$ mouse model to assess the role of FoxO1-S253 in control of glucose homeostasis and demonstrated that impairment of FoxO1 phosphorylation at S253 plays a role in HGP and pancreatic function. The homozygous FoxO1-S253$^{A/A}$ mice displayed the following: (i) normal body weight, slightly increased postprandial blood glucose, and decreased fasting blood glucose; (ii) elevated blood insulin by twofold, reduced blood glucagon by 40%, and a significantly decreased ratio of pancreatic α-cells/β-cells; and (iii) increased FoxO1 stability and HGP. Thus, our data demonstrated that blockage of FoxO1 phosphorylation at S253 *in vivo* resulted in a unique pattern of metabolic dysregulation.

The role of FoxO1 in glucose metabolism in hepatocytes is well studied (8, 29–32), but this study provided genetic evidence to decipher the role of FoxO1 phosphorylation at S253 in control of HGP, glucose homeostasis, and pancreatic biology *in vivo*. In the feeding state, blood glucose of FoxO1-S253$^{A/A}$ mice increased by 15% compared with control mice, suggesting that insulin suppression on HGP was blocked by FoxO1-S253A point mutation. The enhanced gluconeogenesis by the point mutation is further supported by the PTT in mice and *in vitro* analysis of primary hepatocytes isolated from mice, excluding the potential influences of endocrine hormones altered *in vivo*, including insulin and glucagon.

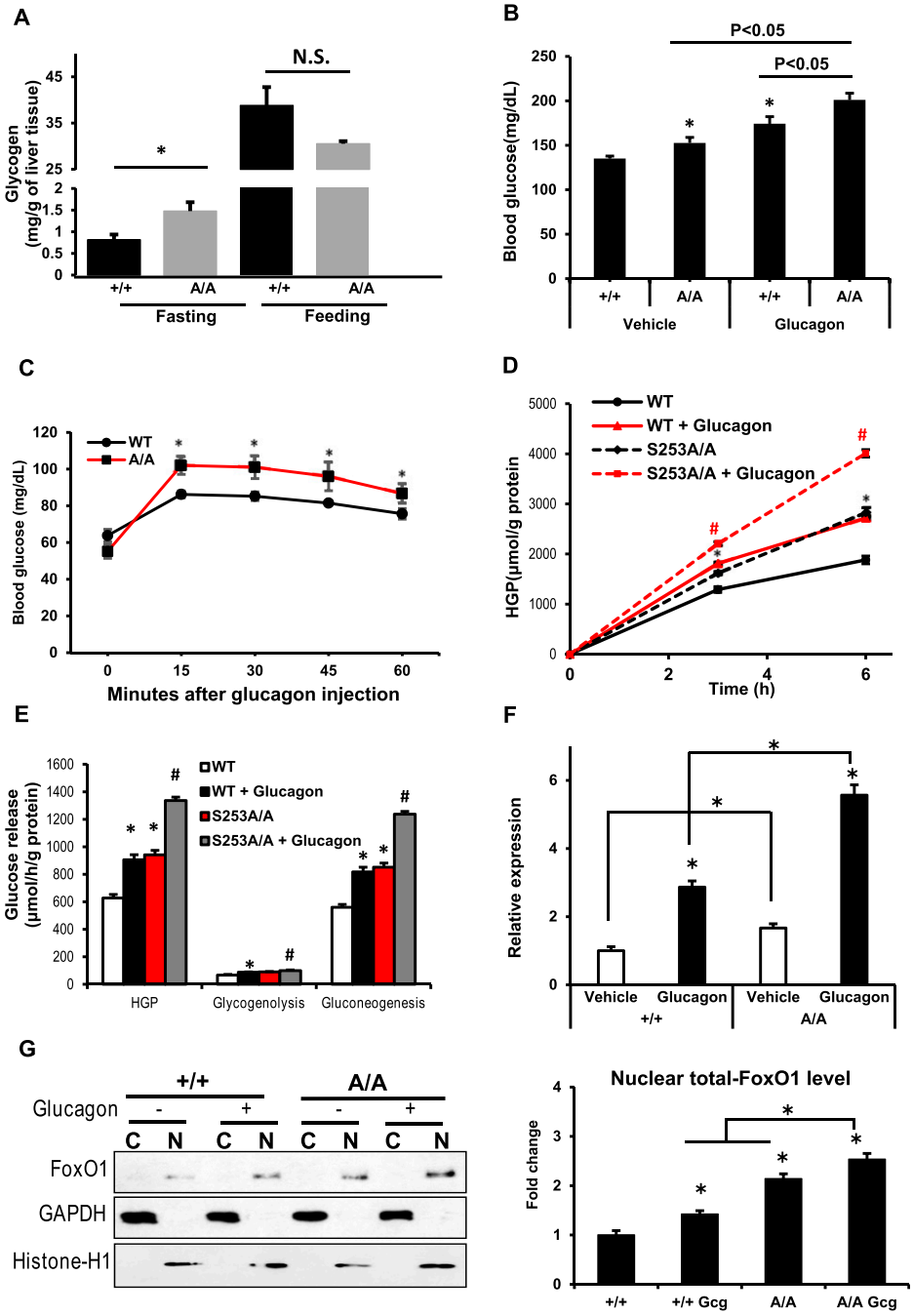

Figure 5. FoxO1-S253$^{A/A}$ mice exhibit impaired glucagon tolerance test and hepatic gene expression. (A) Glycogen concentration in the liver of mice at 16-hour fasting and random-fed states. *$P < 0.05$ vs control, n = 6 mice per group. (B) Blood glucose in random-fed mice injected by glucagon. *$P < 0.05$ vs control, n = 8 per group. (C) Glucagon tolerance tests in control and A/A mice at the age of 12 weeks. Blood glucose was measured in 18-hour unfed mice by 16 μg/kg body weight of glucagon IP injection. *$P < 0.05$ vs control, n = 8 mice per group. (D) HGP assay in primary hepatocytes of control and A/A mice. Cells were stimulated by 100 nM glucagon, and glucose concentrations in culture medium were measured. *$P < 0.05$ WT vs WT + glucagon; $^{\#}P < 0.05$ S253A/A vs S253A/A + glucagon, n = 3 experiments. (E) HGP, glycogenolysis, and gluconeogenesis were measured in the primary hepatocytes. *$P < 0.05$ vs WT; $^{\#}P < 0.05$ vs A/A, n = 3 experiments. (F) Gene-expression levels of G6pc were measured in primary hepatocytes by real-time PCR. Data presented as average of triplicate determinations from control and A/A or 100 nM glucagon stimulation for 8 hours. *$P < 0.05$, n = 3. PCR primer sequences are cyclophilin 5′-ctaaagcatacaggtcctggcatcttg-3′ and 5′-tgccatccagccattcagtcttg-3′; G6pc are 5′-cattgtggcttccttggtcc-3′ and 5′-ggcagtatgggataagactg-3′. (G) Nuclear (N) and cytoplasmic (C) proteins were extracted from control and A/A primary hepatocytes, with or without 100 nM glucagon (Gcg) stimulation for 30 minutes. Cytoplasmic proteins (100 μg) and 20 μg nuclear proteins were subjected to SDS-PAGE and Western blot analysis. Quantification of nuclear FoxO1 was normalized by histone-H1 with analyses from ImageJ. *$P < 0.05$ vs control, n = 3 experiments. GAPDH, glyceraldehyde 3-phosphate dehydrogenase; N.S., no significance.

An increase of HGP and blood glucose during feeding conditions may also contribute to pancreatic β-cell secretion of insulin, which inhibits glycogenolysis and/or stimulates glycogen synthesis, compensating for further elevation of blood glucose in A/A mice. However, with the elevated level of insulin by twofold in KI mice, also observed during the fasting state, even blood glucose was slightly reduced by 10%, which encouraged us to examine pancreatic α-cells and glucagon levels. Compared with control mice, the decreased blood glucose in A/A mice during the fasting state can be a result of higher levels of insulin that promotes glycogen synthesis and lower levels of glucagon for attenuation of gluconeogenesis (Fig. 6). The key downstream effectors of glucagon include cAMP content and cAMP response element-binding protein functionality at gene transcriptional levels (33). A potential reduction of cAMP and cAMP response element-binding protein functionality in the liver of A/A mice may also play a role in attenuation of hepatic gluconeogenesis gene expression. Importantly, we have recently discovered a mechanism by which glucagon and cAMP-dependent protein kinase (protein kinase A) promote FoxO1 nuclear localization and functionality in the liver via FoxO1-Ser273 phosphorylation (34). Another independent study also indicates that glucagon induces Foxo1 nuclear localization and HGP via a Ca^{2+}/calmodulin-dependent protein kinase II on multiple phosphorylation sites of Foxo1 (35). Moreover, HGP is also controlled by the substrate availability through extrahepatic tissues, in addition to hepatic gene transcriptional programming. For example, lipolysis suppression in the peripheral fat tissues, as well as in the liver, by high-insulin or low-glucagon levels, can result in a reduction of substrates of gluconeogenesis or acetyl-coenzyme A content that reduces hepatic pyruvate carboxylase activity and then gluconeogenesis (36, 37). This may be the case in the A/A mice in that hepatic pyruvate and blood triglycerides were reduced (data not shown), and HGP elevated significantly, as we observed in the PTT. The alteration of hepatic substrate availability can be related to lower glucagon and higher insulin levels in the blood of A/A mice when compared with control mice.

FoxO1 also plays a role in the pancreatic β-cell differentiation and function, but its role in control of α-cells is unclear, even though its expression in adulthood is very low (2, 38). In general, FoxO1 inhibits cell proliferation and induces apoptosis in a number of cells (4). Suppression of FoxO1 in the pancreatic β-cells promotes survival and cell mass when IRS2 is absent (10). Conversely, FoxO1 in the pancreas also promotes pancreatic progenitor cell differentiation by inducing expression of MafA and Neurod1 gene expression (39). A recent study showed that FoxO1 deficiency in pancreatic β-cells promoted de-differentiation of β-cells into the progenitor-like cells, including neurogenin-3 and Oct4 gene expression, and even the α-cells (2). Our results from the FoxO1-S253$^{A/A}$ mice suggest that FoxO1-S253$^{A/A}$ enhances β-cell function and blood insulin, whereas it decreases α-cell numbers and blood glucagon, as indicated by the lower ratio of α-cells/β-cells. The potential mechanism of pancreatic α-cell suppression and β-cell promotion by FoxO1-S253$^{A/A}$ is unclear, but our data indicate that the FoxO1-S253$^{A/A}$ mutant pancreas had increased pancreatic mass and expression of marker genes for β-cells and pancreatic progenitor cells and reduced marker genes for α-cells; even insulin and glucagon gene expression in the pancreas of mutant pancreas is not significantly altered. The reason for the increase in pancreas weight in FoxO1-S253$^{A/A}$ mice is unclear. It may relate to an increase in insulin that serves as a paracrine factor promoting the growth in size of pancreatic tissue or differentiation of a different pancreatic cell population. Thus, FoxO1-S253 de-phosphorylation may reflect a molecular modification on FoxO1 as compensation for pancreatic plasticity during development of insulin resistance, where insulin secretion from the β-cells generally suppresses glucagon secretion from the α-cells.

Our data indicate that FoxO1-S253 de-phosphorylation regulates pancreatic plasticity, and the clinical relevance of this study is high. Here, we proposed a model for the role of FoxO1-S253 in

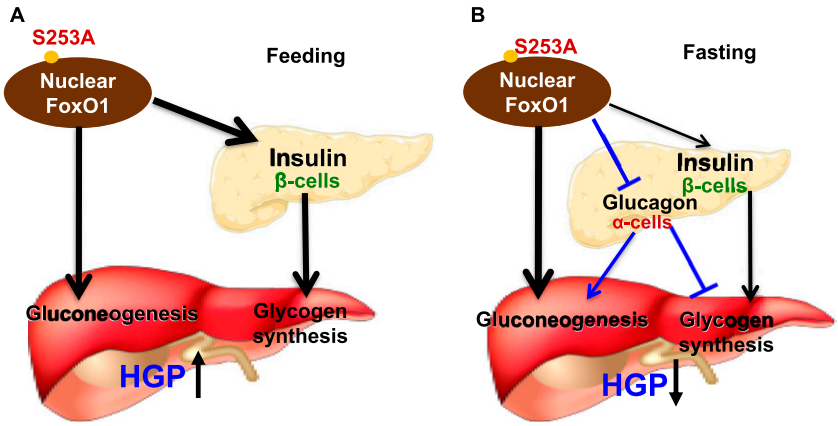

Figure 6. Dephosphorylation of FoxO1-S253 in FoxO1-S253$^{A/A}$ mice regulates hepatic gluconeogenesis, glycogen metabolism, and pancreatic plasticity. (A) FoxO1-S253 de-phosphorylation controls insulin and glucagon production in the pancreas, regulating liver glucose metabolism in the feeding state, resulting in an increase of blood glucose. (B) At the fasting state, where blood glucagon decreases, reducing the blood glucose. →, stimulation; ⊣, inhibition.

the pancreas and liver in control of glucose metabolism during development of insulin resistance. In the pancreas of adulthood, FoxO1-S253 was phosphorylated and suppressed by feeding conditions upon insulin secretion but was moderately activated on fasting conditions by de-phosphorylation when insulin decreases, and glucagon increases. This may be important for β-cell maintenance and function by FoxO1-S253 de-phosphorylation at the fasting condition, where FoxO1 is functional for β-cell identity and maintenance when insulin secretion reduced. The β-cells are insulin responsive, and FoxO1 deficiency was observed in the islets of individuals of T2D, even though in other peripheral tissues, such as the liver, FoxO1 is activated (40). We speculate that hyperinsulinemia promotes FoxO1 cytoplasmic localization, degradation, or deficiency upon early development of T2D, particularly in β-cells, promoting β-cell de-differentiation into the α-cells in the pancreas. Several lines of evidence over the past decades support the concept by the following: (i) β-cells are derived from existing β-cells based on genetic-tracing studies (41, 42); (ii) β-cell mass, function, and insulin secretion decrease, and hyperglucagonemia develops in late-phase T2D in patients; and (iii) a complete FoxO1 deficiency in β-cells promotes β-cell de-differentiation to progenitor-like or α-cells for glucagon production (43). Thus, we predict that increase of glucagon, in addition to other metabolic stress, may be a result of hyperinsulinemia, FoxO1 deficiency in β-cells, and FoxO1 activation in other tissues, such as liver in patients with T2D. Indeed, the pancreas mass increased in KI mice, probably by increased progenitor cell populations, as we predicted, with limited and little direct evidence in which elevated insulin secretion may have a role in the enhancement of the pancreas mass with other mechanisms. The KI mice showed an increase in insulin and a decrease in glucagon at the both fasting and feeding conditions, suggesting that the A/A mutation may have key roles in maintaining β-cell function/insulin secretion and directing to progenitor cell differentiation, increasing pancreas mass, whereas restraining its de-differentiation to the α-cells.

Hyperactivation of FoxO1 by multiple mechanisms contributes to development of diabetes from insulin resistance. At the physiological level, phosphorylation of FoxO1-S253 markedly decreases in the liver during the fasting state when blood insulin decreases, whereas glucagon increases, promoting gluconeogenesis. The FoxO1-S253$^{A/A}$ mutation in hepatocytes promotes FoxO1 stability. However, an additional activation mechanism is required for the enhancement of the FoxO1 ability at gene transcriptional levels. In this study, we provide that an additional activation of FoxO1 by glucagon may play a critical role in FoxO1 enhancing HGP and the elevation of blood glucose. Consistent with the previous reports (34, 35), we showed that glucagon significantly stimulated FoxO1 nuclear localization and stability. Of note is that the total Foxo1 protein level in the A/A pancreas decreased by 40% compared with that of the WT pancreas (data not shown), which might relate to the effect of a lower glucagon level in the mutant mice. In diabetic conditions, de-phosphorylation of FoxO1-S253 is present in tissues of subjects with T2D when insulin resistance occurs, failing to activate Akt, and hyperglucagonemia develops (34, 44, 45). This study showed that a moderate activation of FoxO1 via de-phosphorylation of S253 alone is not sufficient for induction of diabetes in mice, unexpectedly, as a compensatory benefit to the metabolism for maintaining insulin sensitivity with higher EE and lower physical activity. The mechanism may relate to an increase in gene expression of Irs2 in tissues, such as liver (data not shown).

In the KI mice, the feeding blood glucose and insulin increase, suggesting that an insulin-dominant role in suppression of gluconeogenesis is attenuated by A/A liver when blood glucagon decreases (Fig. 6A). However, the fasting blood glucose and glucagon decrease in the KI mice, suggesting that a glucagon-dominant role in stimulation of gluconeogenesis is attenuated, accompanied with an increase of insulin that can stimulate glycogen synthesis or inhibit glycogenolysis (Fig. 6B).

In addition to liver and pancreas, we do not exclude the possibility that other tissues with the FoxO1-S253$^{A/A}$ mutation can be involved in the regulation of the blood glucose and energy metabolism. For example, FoxO1 in hypothalamic neurons increases food intake and/or increases EE (46). FoxO1- S253$^{A/A}$ represents a combination of outcome of contribution from all tissues in the whole body. Taken together, our data provide genetic and cellular evidence for a fundamental mechanism by which impairment of FoxO1 phosphorylation at S253 can alter blood glucose, at least via the liver and pancreas, involving the control of hormones and pancreatic plasticity. Our findings may provide a strategy in targeting FoxO1 and its interaction with other factors for conquering T2D in the future.

Acknowledgments

The authors thank members of the S.G. and M.F.W. laboratories for discussion of the data, Vanderbilt University Mouse Metabolic Phenotyping Center for hyperinsulinemic-euglycemic clamp assay and data analysis (Li Kang, DK059637), and Children's Hospital Boston, Mouse Genetics Facility, for performing microinjection of the gene-targeting vector and providing the ES cells for screening. Parts of this study were presented at the 75th Scientific Session of the American Diabetes Association (ADA), Chicago, Illinois, 5–9 June 2013, and the 78th

Scientific Session of the ADA, Orlando, Florida, 22–26 June 2018.

Financial Support: This work was supported by grants from the National Institutes of Health (RO1 DK095118 and R56 DK118334-01), American Diabetes Association Career Development Award (1-15-CD-09), American Heart Association (BGIA-7880040), Faculty Start-up from Texas A&M University AgriLife Research, and US Department of Agriculture National Institute of Food and Agriculture (Hatch 1010958; all to S.G.) and National Natural Science Foundation of China (Grants 81471067 to K.Z., 81471022 to Y.Q., and 81300681 to L.L.).

Author Contributions: K.Z., X.G., H.Y., Y.W., Q.P., J.Z.S., X.L., Y.C., L.L., Y.Q., Z.X., W.X., W.Z., D.T., L.H., D.V., Y.S., and S.G. performed experiments. X.G. and S.G. wrote the manuscript. H.Y., H.Z., M.F.W., and Y.S. revised the manuscript. S.G. is a recipient of the 2015 American Diabetes Association Research Excellence Thomas R. Lee Award and is the guarantor of this work and as such, had full access to all of the data in the study and takes responsibility for the integrity of the data and accuracy of the data analysis.

Correspondence: Shaodong Guo, PhD, Department of Nutrition and Food Science, College of Agriculture and Life Sciences, Texas A&M University, 123A Cater-Mattil Hall, College Station, Texas 77843. E-mail: shaodong.guo@tamu.edu.

Disclosure Summary: The authors have nothing to disclose.

References

1. Lee S, Dong HH. FoxO integration of insulin signaling with glucose and lipid metabolism. *J Endocrinol*. 2017;**233**(2):R67–R79.
2. Talchai C, Xuan S, Lin HV, Sussel L, Accili D. Pancreatic β cell dedifferentiation as a mechanism of diabetic β cell failure. *Cell*. 2012;**150**(6):1223–1234.
3. Bensellam M, Jonas JC, Laybutt DR. Mechanisms of β-cell dedifferentiation in diabetes: recent findings and future research directions. *J Endocrinol*. 2018;**236**(2):R109–R143.
4. Guo S. Insulin signaling, resistance, and the metabolic syndrome: insights from mouse models into disease mechanisms. *J Endocrinol*. 2014;**220**(2):T1–T23.
5. Guo S, Copps KD, Dong X, Park S, Cheng Z, Pocai A, Rossetti L, Sajan M, Farese RV, White MF. The Irs1 branch of the insulin signaling cascade plays a dominant role in hepatic nutrient homeostasis. *Mol Cell Biol*. 2009;**29**(18):5070–5083.
6. Dong XC, Copps KD, Guo S, Li Y, Kollipara R, DePinho RA, White MF. Inactivation of hepatic Foxo1 by insulin signaling is required for adaptive nutrient homeostasis and endocrine growth regulation. *Cell Metab*. 2008;**8**(1):65–76.
7. Qi Y, Guo X, Guo S. Insulin resistance in obesity. In: Ahima R, ed. *Metabolic Syndrome: A Comphensive Textbook*. Cham, Switzerland: Springer International; 2016:479–504.
8. Zhang K, Li L, Qi Y, Zhu X, Gan B, DePinho RA, Averitt T, Guo S. Hepatic suppression of Foxo1 and Foxo3 causes hypoglycemia and hyperlipidemia in mice. *Endocrinology*. 2012;**153**(2):631–646.
9. Zhang J, Ou J, Bashmakov Y, Horton JD, Brown MS, Goldstein JL. Insulin inhibits transcription of IRS-2 gene in rat liver through an insulin response element (IRE) that resembles IREs of other insulin-repressed genes. *Proc Natl Acad Sci USA*. 2001;**98**(7):3756–3761.
10. Kitamura T, Nakae J, Kitamura Y, Kido Y, Biggs WH III, Wright CV, White MF, Arden KC, Accili D. The forkhead transcription factor Foxo1 links insulin signaling to Pdx1 regulation of pancreatic beta cell growth. *J Clin Invest*. 2002;**110**(12):1839–1847.
11. Rena G, Guo S, Cichy SC, Unterman TG, Cohen P. Phosphorylation of the transcription factor forkhead family member FKHR by protein kinase B. *J Biol Chem*. 1999;**274**(24):17179–17183.
12. Guo S, Rena G, Cichy S, He X, Cohen P, Unterman T. Phosphorylation of serine 256 by protein kinase B disrupts transactivation by FKHR and mediates effects of insulin on insulin-like growth factor-binding protein-1 promoter activity through a conserved insulin response sequence. *J Biol Chem*. 1999;**274**(24):17184–17192.
13. Huang H, Regan KM, Wang F, Wang D, Smith DI, van Deursen JM, Tindall DJ. Skp2 inhibits FOXO1 in tumor suppression through ubiquitin-mediated degradation. *Proc Natl Acad Sci USA*. 2005;**102**(5):1649–1654.
14. Matsuzaki H, Daitoku H, Hatta M, Tanaka K, Fukamizu A. Insulin-induced phosphorylation of FKHR (Foxo1) targets to proteasomal degradation. *Proc Natl Acad Sci USA*. 2003;**100**(20):11285–11290.
15. Cheng Z, Guo S, Copps K, Dong X, Kollipara R, Rodgers JT, Depinho RA, Puigserver P, White MF. Foxo1 integrates insulin signaling with mitochondrial function in the liver. *Nat Med*. 2009;**15**(11):1307–1311.
16. RRID:AB_2106495, https://scicrunch.org/resolver/AB_2106495.
17. RRID:AB_2106814, https://scicrunch.org/resolver/AB_2106814.
18. RRID:AB_329831, https://scicrunch.org/resolver/AB_329831.
19. RRID:AB_561438, https://scicrunch.org/resolver/AB_561438.
20. RRID:AB_561053, https://scicrunch.org/resolver/AB_561053.
21. RRID:AB_2223172, https://scicrunch.org/resolver/AB_2223172.
22. RRID:AB_675641, https://scicrunch.org/resolver/AB_675641.
23. Rossi M, Zhu L, McMillin SM, Pydi SP, Jain S, Wang L, Cui Y, Lee RJ, Cohen AH, Kaneto H, Birnbaum MJ, Ma Y, Rotman Y, Liu J, Cyphert TJ, Finkel T, McGuinness OP, Wess J. Hepatic Gi signaling regulates whole-body glucose homeostasis. *J Clin Invest*. 2018;**128**(2):746–759.
24. Lin X, Taguchi A, Park S, Kushner JA, Li F, Li Y, White MF. Dysregulation of insulin receptor substrate 2 in beta cells and brain causes obesity and diabetes. *J Clin Invest*. 2004;**114**(7):908–916.
25. Bruschetta G, Jin S, Kim JD, Diano S. Prolyl carboxypeptidase in Agouti-related peptide neurons modulates food intake and body weight. *Mol Metab*. 2018;**10**:28–38.
26. Chen J, Zhang Z, Wang N, Guo M, Chi X, Pan Y, Jiang J, Niu J, Ksimu S, Li JZ, Chen X, Wang Q. Role of HDAC9-FoxO1 axis in the transcriptional program associated with hepatic gluconeogenesis. *Sci Rep*. 2017;**7**(1):6102.
27. Pradhan G, Wu CS, Han Lee J, Kanikarla P, Guo S, Yechoor VK, Samson SL, Sun Y. Obestatin stimulates glucose-induced insulin secretion through ghrelin receptor GHS-R. *Sci Rep*. 2017;**7**(1):979.
28. Guo S, Dunn SL, White MF. The reciprocal stability of FOXO1 and IRS2 creates a regulatory circuit that controls insulin signaling. *Mol Endocrinol*. 2006;**20**(12):3389–3399.
29. Haeusler RA, Han S, Accili D. Hepatic FoxO1 ablation exacerbates lipid abnormalities during hyperglycemia. *J Biol Chem*. 2010;**285**(35):26861–26868.
30. Altomonte J, Richter A, Harbaran S, Suriawinata J, Nakae J, Thung SN, Meseck M, Accili D, Dong H. Inhibition of Foxo1 function is associated with improved fasting glycemia in diabetic mice. *Am J Physiol Endocrinol Metab*. 2003;**285**(4):E718–E728.
31. Li X, Monks B, Ge Q, Birnbaum MJ. Akt/PKB regulates hepatic metabolism by directly inhibiting PGC-1alpha transcription coactivator. *Nature*. 2007;**447**(7147):1012–1016.
32. Estall JL. The Foxo family: partners in crime or silent heroes. *Endocrinology*. 2012;**153**(2):549–551.
33. Altarejos JY, Montminy M. CREB and the CRTC co-activators: sensors for hormonal and metabolic signals. *Nat Rev Mol Cell Biol*. 2011;**12**(3):141–151.
34. Wu Y, Pan Q, Yan H, Zhang K, Guo X, Xu Z, Yang W, Qi Y, Guo CA, Hornsby C, Zhang L, Zhou A, Li L, Chen Y, Zhang W, Sun Y, Zheng H, Wondisford F, He L, Guo S. Novel Mechanism of Foxo1 phosphorylation in glucagon signaling in control of glucose homeostasis. *Diabetes*. 2018;**67**(11):2167–2182.

35. Ozcan L, Wong CC, Li G, Xu T, Pajvani U, Park SK, Wronska A, Chen BX, Marks AR, Fukamizu A, Backs J, Singer HA, Yates JR III, Accili D, Tabas I. Calcium signaling through CaMKII regulates hepatic glucose production in fasting and obesity. *Cell Metab*. 2012;**15**(5):739–751.
36. Petersen MC, Vatner DF, Shulman GI. Regulation of hepatic glucose metabolism in health and disease. *Nat Rev Endocrinol*. 2017;**13**(10):572–587.
37. Titchenell PM, Quinn WJ, Lu M, Chu Q, Lu W, Li C, Chen H, Monks BR, Chen J, Rabinowitz JD, Birnbaum MJ. Direct hepatocyte insulin signaling is required for lipogenesis but is dispensable for the suppression of glucose production. *Cell Metab*. 2016;**23**(6):1154–1166.
38. Kitamura T. The role of FOXO1 in β-cell failure and type 2 diabetes mellitus. *Nat Rev Endocrinol*. 2013;**9**(10):615–623.
39. Kitamura YI, Kitamura T, Kruse JP, Raum JC, Stein R, Gu W, Accili D. FoxO1 protects against pancreatic beta cell failure through NeuroD and MafA induction. *Cell Metab*. 2005;**2**(3):153–163.
40. Guo S, Dai C, Guo M, Taylor B, Harmon JS, Sander M, Robertson RP, Powers AC, Stein R. Inactivation of specific β cell transcription factors in type 2 diabetes. *J Clin Invest*. 2013;**123**(8):3305–3316.
41. Dor Y, Brown J, Martinez OI, Melton DA. Adult pancreatic beta-cells are formed by self-duplication rather than stem-cell differentiation. *Nature*. 2004;**429**(6987):41–46.
42. Pagliuca FW, Melton DA. How to make a functional β-cell. *Development*. 2013;**140**(12):2472–2483.
43. Talchai SC, Accili D. Legacy effect of Foxo1 in pancreatic endocrine progenitors on adult β-cell mass and function. *Diabetes*. 2015;**64**(8):2868–2879.
44. He L, Sabet A, Djedjos S, Miller R, Sun X, Hussain MA, Radovick S, Wondisford FE. Metformin and insulin suppress hepatic gluconeogenesis through phosphorylation of CREB binding protein. *Cell*. 2009;**137**(4):635–646.
45. Edgerton DS, Cherrington AD. Glucagon as a critical factor in the pathology of diabetes. *Diabetes*. 2011;**60**(2):377–380.
46. Ren H, Orozco IJ, Su Y, Suyama S, Gutiérrez-Juárez R, Horvath TL, Wardlaw SL, Plum L, Arancio O, Accili D. FoxO1 target Gpr17 activates AgRP neurons to regulate food intake [published correction appears in *Cell*. 2012;**153**(5):1166]. *Cell*. 2012;**149**(6):1314–1326.